A comparison of the reaction-diffusion kinetics between model-EUV polymer and molecular-glass photoresists [§]

Shuhui Kang[1], Kristopher Lavery[1], Kwang-Woo Choi[1,2], Vivek M. Prabhu[1], Wen-li Wu[1], Eric K. Lin[1], Anuja De Silva[3], Nelson Felix[3], Christopher Ober[3],

[1]Polymers Division, National Institute of Standards and Technology, 100 Bureau Dr, Gaithersburg, MD 20899
[2]Intel Corporation, Santa Clara, CA
[3] Cornell University, Materials Science & Engineering, 310 Bard Hall, Ithaca, NY 14853-1501

ABSTRACT

It has been recently postulated that sub-22 nm photolithography with polymeric photoresists has reached a materials design barrier due to its large molecular mass and distribution. In this argument, the “pixel” size, which is related to the smallest molecular unit, determines the feature fidelity and resolution of the lithographic process. This hypothesis remains unproven, but molecular glass photoresists can provide a test because they can share similar chemical functionality to polymer resists, but with low molecular mass and a monodisperse molecular mass distribution. The low molecular mass leads to the smaller pixel size compared to the radius of gyration of the polymer photoresist. In this work, we compare the deprotection reaction-diffusion kinetics of a common photoacid generator in a polymer and molecular glass resist with similar resist chemistry to elucidate effects of molecular architecture on photoresist performance. We determine the mechanism of reaction, photoacid trapping behavior, and diffusivity by measuring and comparing the reaction kinetics parameters as a function of temperature and exposure dose. These results permit an analysis of the latent image formation which is a crucial factor in resolution and line-edge roughness. Further, knowledge of the reaction-diffusion parameters of each type of resist provides a quantitative approach to predict line-space features, crucial for design for resolution-enhancement features.

Key words: Diffusion coefficient; photoacid; photoresist; kinetics; FTIR; Molecular glass

1. INTRODUCTION

The photoacid catalyzed deprotection reaction and resulting reaction-diffusion kinetics is at the root cause of current projection lithography feature limitations with chemically amplified photoresists. Measurements of the reaction kinetics constants and photoacid diffusion constant would allow a predictive approach to line-edge feature critical dimensions. This approach should provide physically-based parameters which may qualify, or aide in the interpretation of parameters determined empirically by photolithography process window experiments. More specifically, current challenges are in designing resists that faithfully reproduce the resolution-enhancement features in masks. These features require physical parameters that produce an understanding of sub-32 nm imaging. Therefore, measurements are required that provide sensitivity to nanometer-scale acid diffusion lengths in model EUV (Extreme Ultraviolet) photoresist materials.

In this study, we developed infrared spectroscopy methods to quantitatively determine the deprotection reaction kinetics using two approaches; a zero-gradient and one-dimensional gradient method. The zero-gradient method determines the appropriate chemical reaction model and quantifies the reaction kinetics constants. The one-dimensional gradient model measures the photoacid diffusion coefficient as the photoacid reaction-diffusion front moves from an initial sharp step

---

[§] Official contribution of the National Institute of Standards and Technology; not subject to copyright in the United States

Advances in Resist Materials and Processing Technology XXV, edited by Clifford L. Henderson,
Proc. of SPIE Vol. 6923, 692317, (2008) · 0277-786X/08/$18 · doi: 10.1117/12.773018

profile that mimics an ideal exposure edge. The reaction kinetics of a common photoacid generator, triphenylsulfonium perfluorobutanesulfonate (TPS-PFBS), in a polymer and molecular glass resist thin films are compared. The effect of reaction kinetics parameters dependence on post-exposure bake temperatures and dose are determined.

2. EXPERIMENTAL[#]

2.1 Materials

Two different architectures of resists: a polymeric photoresist, poly(hydroxystyrene-*co*-*tert*-butylacrylate) or P(HOSt-*co*-tBA)[1] and a *tert*-butoxycarbonyl (t-BOC) protected calix[4]resorcinarene molecular glass material were studied[2]. The P(HOSt-*co*-tBA) had a number average relative molar mass (M_n) = 11,459 g/mol, polydispersity index (PDI) = 1.83, and copolymer composition of 49 % by mole HOSt and 51 % by mole tBA (DuPont Electronic Polymers). The chemical formula and acid deprotection reaction equation are shown in Scheme I and Scheme II. The same photoacid generator, TPS-PFBS was used to directly compare the effect of architecture on the photoacid reaction-diffusion kinetics. When referring to the PAG loadings (or concentration) it will be implied as % by mass from this point forward. We notice that the protection groups do differ, which will lead to a small difference in reaction activation energy; however both materials share phenol functionality. We will compare our results to those in the literature for *t*-BOC protected PHOST, which share the same t-BOC protection chemistry to the molecular resist studied in this paper.

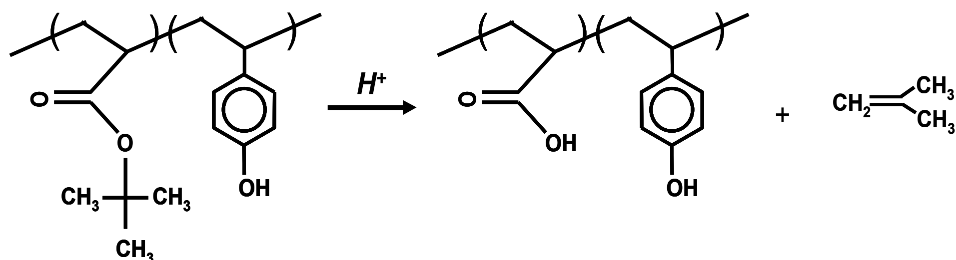

Scheme I: Acid catalyzed deprotection reaction of P(HOSt-*co*-tBA),

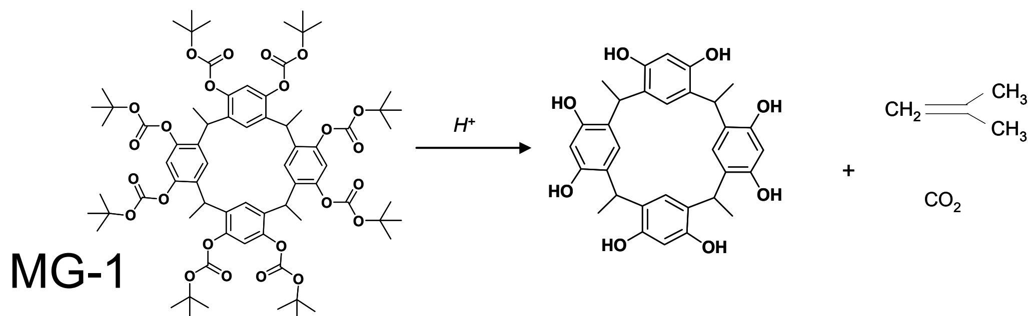

Scheme II: Acid catalyzed deprotection reaction of molecular glass (MG-1) t-BOC protected calix[4]resorcinarene.

2.2 Sample preparation and instrumentation

Two methods of thin film preparation called single layer and bilayer layer. Single-layer methods refer to simply the model photoresist formulation prepared on silicon wafer. The bilayer method involves forming a stacked layer structure

[#] Certain commercial equipment and materials are identified in this paper in order to specify adequately the experimental procedure. In no case does such identification imply recommendations by the National Institute of Standards and Technology nor does it imply that the material or equipment identified is necessarily the best available for this purpose.

of two films on a silicon wafer with high fidelity and no intermixing between the two layers. Both single layer and bilayer films are used in this experiment. In the single layer film, the acid is uniformly distributed, while in the bilayer film, the acid is present only in the top layer. The single layer sample provides the simplest system to study the reaction kinetics to estimate the reaction rate constant, photoacid trapping rate constant or acid loss constants. In the single layer film, the diffusion coefficient is completely coupled with the reaction rate constant because the gradient of photoacid concentration is zero. In order to determine the photoacid diffusion coefficient a well-defined initial acid gradient is necessary to follow the moving photoacid reaction front.

A new poly(dimethylsiloxane) (PDMS) film stamping technique was developed to generate the well-defined acid concentration gradient. In this case a resist film containing photoacid generator (PAG) is prepared upon a PDMS substrate then stamped onto an identical PAG-free resist film at an elevated temperature for 30 s. After the stack cools the PDMS substrate is removed. The primary advantage of this bilayer approach is that only one diffusion media is present. This approach is more convenient than previous double spin coating methods, which do provide high fidelity bilayers, but have severe limitations on finding suitable casting solvents and acid feeder layers that do not share the same polymer media as the bottom layer[3-5]. The PDMS method forms an interface between two identical polymer layers. However, in our case the top layer contains PAG. The interfacial width was determined to be (1 to 2) nm as measured by neutron reflectivity with a bilayer of deuterated and protonated poly(methyl methacrylate). Therefore, the loaded PAG has a nearly perfect step profile within length scales of the interfacial width.

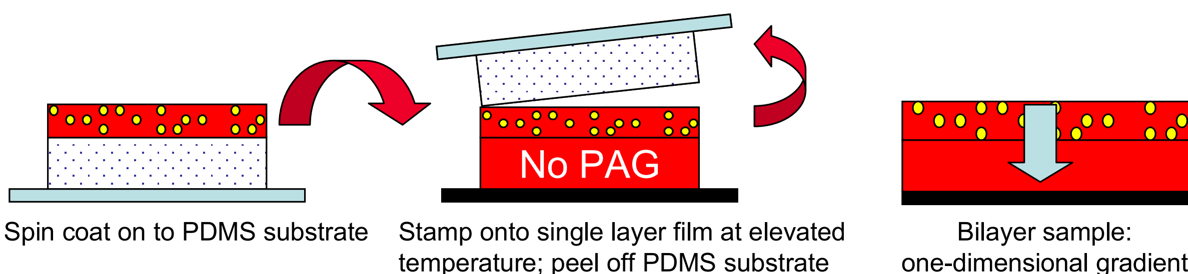

Scheme III. Bilayer sample preparation with the PDMS film transferring technique.

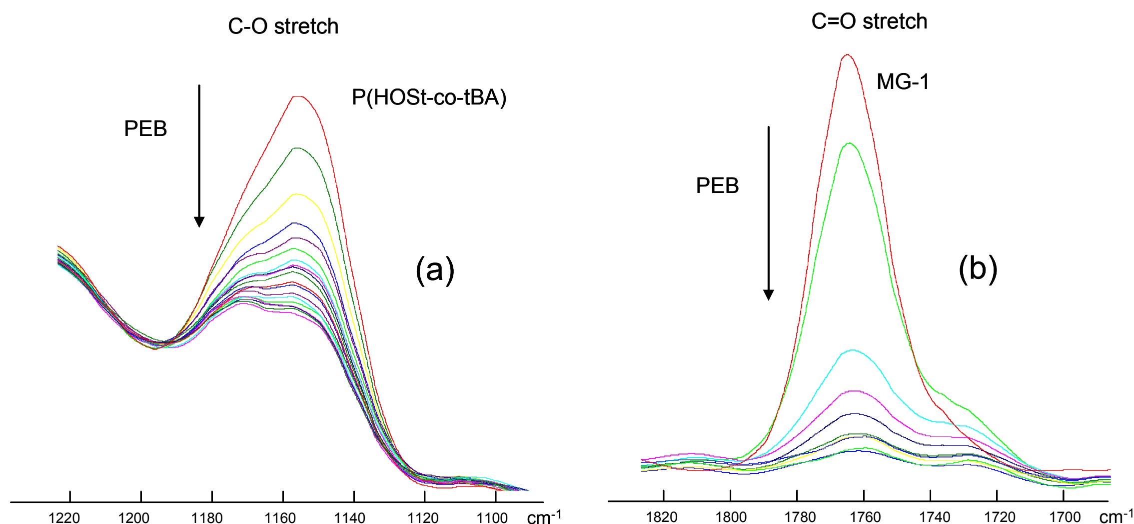

Figure 1. (a) C-O stretching vibrational band evolution during PEB for P(HOSt-*co*-tBA). (b) C=O stretching vibrational band evolution during PEB for MG-1.

The C−O stretching vibrational spectroscopic band around 1160 cm^{-1} is used to quantify the deprotection level of P(HOSt-*co*-tBA), upon PEB (Figure 1a) while the C=O stretching vibrational spectroscopic band around 1760 cm^{-1} is used for MG-1 (Figure 1b).

All the Fourier transform infrared (FTIR) spectra were collected with Bomem FTLA 2000 with reflection mode at 16 cm^{-1} resolution. The silicon wafers were coated with Au to increase IR reflectivity and mounted on a preheated hot-stage though vacuum contact. Film thicknesses were measured with J.A. Woollam IR spectroscopic ellipsometer with error (one standard deviation) in between (1 to 2) nm based on a calibration with film thickness determined by X-ray reflectivity.

2.3 Reaction-diffusion modeling and methodology

The details of the modeling approach used are discussed elsewhere, but we provide a brief summary[6,7]. There are three mains parts in this kinetics model. The first part uses Dill's equation to describe the acid generation process. The photoacid concentration H is exponentially dependent on the UV exposure E shown in Equation 1. The [PAG] is the initial photoacid generator loading and the C is the Dill's parameter which dependent upon the type of PAG and the UV wavelength. The second part (Equation 2) describes the deprotection reaction rate such that the rate of change in deprotection level ϕ is determined by a first order reaction between resist protected species (1-ϕ) and the photoacid concentration where k_P is the reaction rate constant. The third part (Equation 3) describes the transport properties of photoacid which is typically non-Fickian because the acid can be trapped with rate constant k_T. D_H is the diffusion coefficient for photoacid. In the present case both experimentally and modeling, there are no added quenchers.

$$H = [PAG]\left(1 - e^{-CE}\right) \quad (1)$$

$$\frac{d\phi}{dt} = k_P H (1 - \phi) \quad (2)$$

$$\frac{\partial H}{\partial t} = D_H \nabla^2 H - k_T H \phi \quad (3)$$

The photacid trapping mechanism has been discussed in our previous work[6-9]. The photoacids could be trapped by the reaction products through strong hydrogen bonding interactions. The trapping is dictated by local deprotection level such that with higher deprotection level, the stronger the trapping effect. However in the literature[10,11], this was treated as an acid loss mechanism which is independent of deprotection level and modeled as $-k_L H$ where k_L is called acid loss constant and its inverse characterizes photoacid lifetime. There is almost no difference in describing the single layer film system with these two models except that the k_T is usually several times larger than k_L because the deprotection level is always less than one, while it appears necessary to use the trapping mechanism of Equation 3 to describe the deprotection profile at the interface of a bilayer system[12].

If all the parameters and the initial conditions are known, the deprotection level ϕ can be solved at any given post-exposure bake (PEB) time and any position of the sample from the system of equations. A Matlab program was written to calculate the zero-gradient (single layer) and one-dimensional gradient (bilayer) structure. Using FTIR, we can measure with excellent accuracy and low noise level, the time evolution of the average deprotection.

3. RESULTS AND DISCUSSION

3.1 Reaction and loss constants

Figure 2a and 2b show the single layer film deprotection level change with temperature and PEB time for P(HOSt-*co*-tBA) and MG-1 measured with FTIR . It can be seen that the deprotection level increases with PEB time and temperature (60 °C to 100 °C). A significant feature for these curves is that deprotection saturates below completion, or the reaction nearly stops. Using the kinetics model described previously, the reaction rate constant and acid trapping loss constant for various temperatures were determined as summarized in Table I and Figure 3. Both k_p and k_L are larger for MG-1 than P(HOSt-*co*-tBA) at equal PEB temperatures. This could be due to the lower glass transition temperature (T_g) for MG-1 (T_g = 115 °C) than P(HOSt-*co*-tBA) (T_g = 150 °C). Another possibility is based upon the resist chemistry which favors

hydrogen bonding between the photoacid and the polar group in the resist. The photoacid is a strong hydrogen-bond donor, while the phenol on PHOSt and/or the carbonyl are hydrogen bond acceptors. In MG-1 the C=O is mostly shielded by the protection groups and not easily accessible and do not participate in hydrogen bonding as determined by FTIR. However, the hydroxyls in the P(HOSt-*co*-tBA) copolymer are accessible. The interaction with these polar groups can slow down the diffusion of photoacid[13] and its reaction rate which is dictated by acid diffusion[14,15] in these diffusion-controlled systems.

The average acid lifetime is the reciprocal the acid loss constant k_L and reflects how long the acid actively catalyzes the reaction. Table I shows that the photoacid has shorter lifetime in MG-1 than in P(HOSt-*co*-tBA) at a given PEB temperature. It is not quite clear how the acid is lost or trapped in these resist but it could be related due to binding within the cup-like structure, or ordering (crystallization) of the deprotected MG-1 forming a dense packing due to loss of large bulky protecting groups that prevents acid transport.

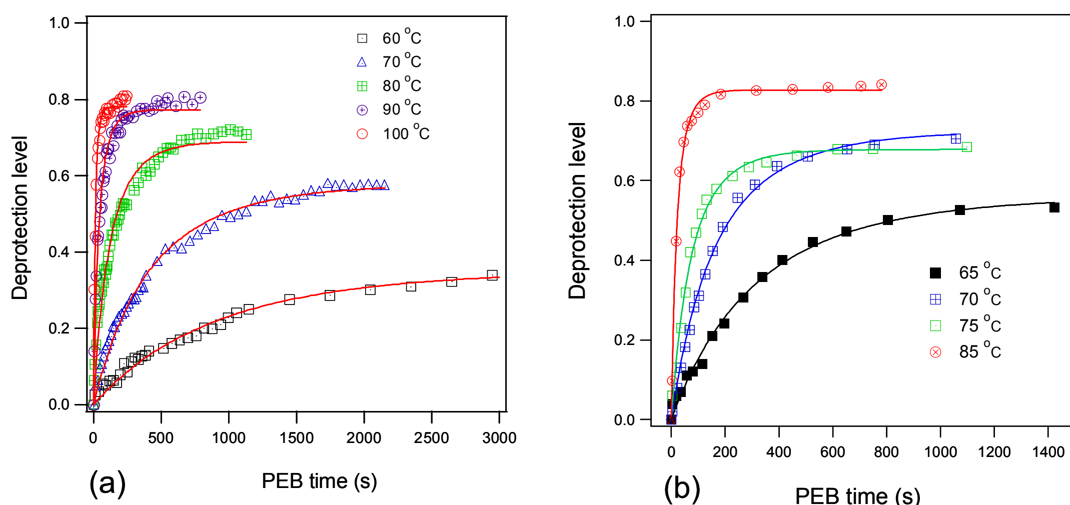

Figure 2. Average deprotection level change in single layers with PEB time and temperature (a) P(HOSt-*co*-tBA) with 2 % PAG loading; (b) MG-1with 1 % PAG loading. Error (one standard deviation) for deprotection quantification is around 0.01~0.02. The solid lines are the fitted curves from the kinetics model.

Table I. Reaction parameters for P(HOSt-*co*-tBA) and MG-1at various PEB temperatures.

P(HOSt-*co*-tBA) (γ=0.02; ρ =1.2g/cm^3; H_0 =0.0257 nm^{-3})			Molecular glass (MG-1) (γ=0.01; ρ =1.2g/cm^3; H_0 =0.0129 nm^{-3})		
PEB [°C]	k_P (nm^{3}s^{-1})	k_L (s^{-1}) / acid lifetime (s)	PEB [°C]	k_P (nm^{3}s^{-1})	k_L (s^{-1}) /acid lifetime (s)
60	0.016	0.00094 / 1064	65	0.14	0.0022 / 454
70	0.058	0.0017 / 588	70	0.36	0.0036 /278
80	0.24	0.0052 / 192	75	0.74	0.0084 / 119
90	0.78	0.014 / 71	85	3.1	0.023 / 43
100	2.6	0.043 / 23			

PAG loading and the initial acid concentration can be converted from formula $[PAG]_0 = H_0 = \gamma \rho N_A / M_{PAG}$

γ is the mass fraction of PAG in resist film; ρ is the mass density of polymer resists; M_{PAG} is the molecular mass of PAG; N_A is Avogadro's constant.

The reaction rate and acid loss constants increase with PEB temperature for both P(HOSt-*co*-tBA) and MG-1. The temperature dependence can be described by an Arrhenius equation $\ln k_P = A - E_a / RT$ to determine the activation energy E_a (Table II) and prefactor (A). The activation energy and prefactor for MG-1 are slightly larger than the P(HOSt-*co*-tBA). Since the activation energy reflects the sensitivity of a resist to temperature change. The higher a

resist's activation energy is, the more sensitive the resist can be to PEB temperature and less stable to temperature variation. The difference in activation energy between two photoresists could be also related to their glass transition temperatures. The closer to T_g the barriers to diffusion are reduced as the polymer matrix gains increased cooperative mobility of a few chain segments. Therefore, from the single layer measurements we understand architecture leads to a quantitative difference in activation energy and photoacid lifetime. The data are of excellent quality to permit such a comparison. However, a better comparison may be made between PBOCSt and MG-1 where the protection chemistry is the same. The prefactor and the activation energy for the reaction rate constants for PBOCSt were measured by FTIR with stochastic simulation modeling[16] are also shown in Table II. It can be seen that molecular glass resist still has larger activation energy and prefactor than polymeric resist PBOCSt.

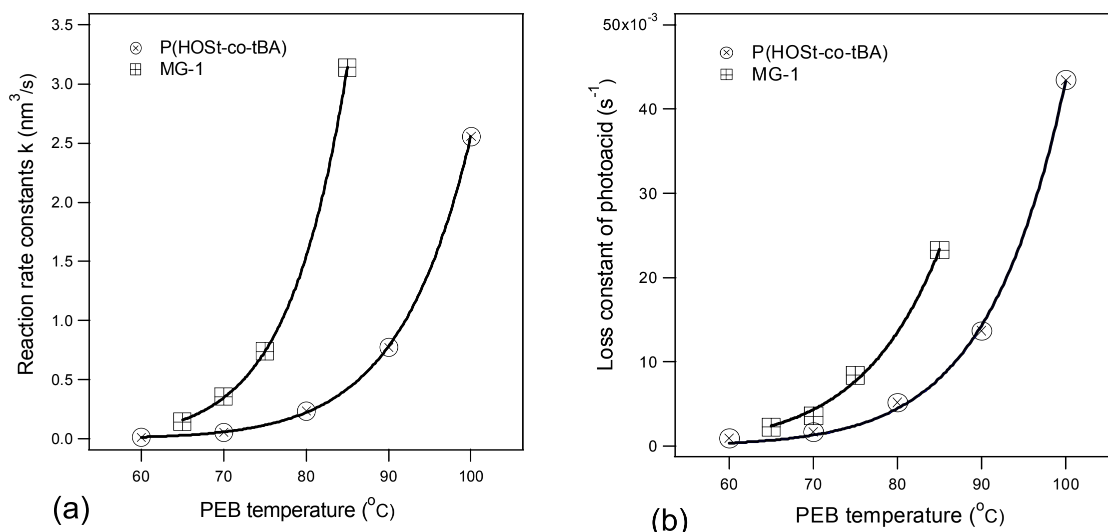

Figure 3. Reaction rate constants (a) and photoacid loss constant (b) for P(HOSt-*co*-tBA) and MG-1at various PEB temperature. The solid lines are fitted curves from Arrhenius model.

Table II. Activation energy of deprotection reaction of photoacid in P(HOST-CO-TBA) and MG-1.

	Reaction rate constant		Photoacid loss constant (s^{-1})	
	A	E_a (kJ/mol)	A	E_a (kJ/mol)
P(HOSt-*co*-tBA)*	43.9±0.3	133.4±1.1	29.1±2.6	124.5±3.7
MG-1*	51.6±0.5	150.1±1.4	34.8±2.4	115.0±7.2
PBOCSt [16] (Houle et. al.)	41.8	119.8		

* Uncertainties are shown one standard deviation from the mean of three measurements

3.2 Photoacid diffusion constant

The diffusion coefficients are determined by simultaneously fitting the FTIR reaction kinetics data to both single layer and bilayer systems. The three kinetics parameters: k_P, k_T, and D_H are extracted in the same fit as shown in the example of Figure 4. It can be seen that the model fit both the single layer and bilayer films well, indicating both systems can be described by the model and are governed by the same kinetics. Here we use the absolute reaction extent instead of the deprotection level. The absolute reaction extent is the deprotection scaled to the acid feeding layer and therefore could be larger than 1.0 for a bilayer film sample. Since the absolute reaction extent is always larger than the corresponding single layer it provides a direct comparison regarding the magnitude of the diffusion coefficient. The results of reaction-diffusion kinetics parameters in P(HOSt-*co*-tBA) at 90 °C PEB are listed in Table 3 for three different samples.

We demonstrate that the PDMS stamping approach is reproducible and the experimental parameters are independent of the stack thickness and initial PAG concentration by comparing 2 % to 5 % TPS-PFBS. This is demonstrated by the small variation in reaction constants and photoacid diffusion constant in Table III.

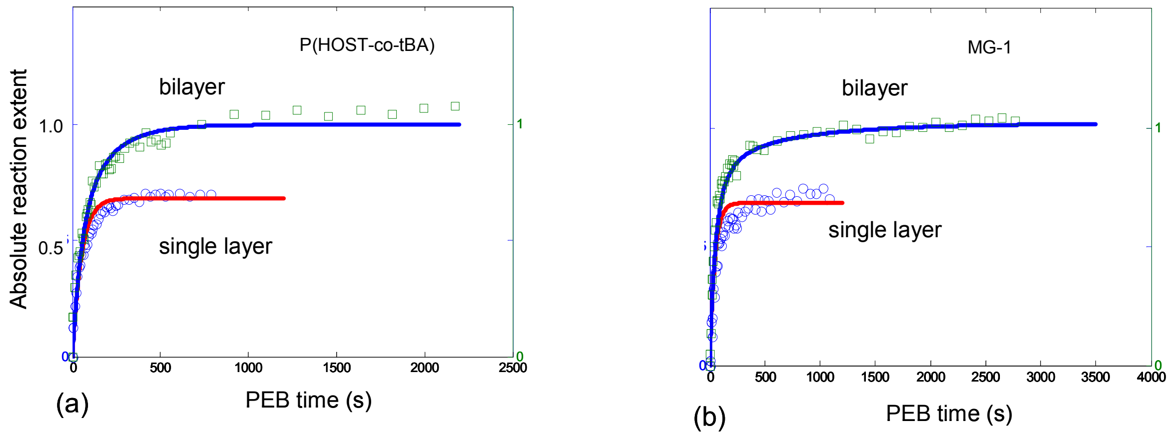

Figure 4. Absolute reaction extent vs. PEB time for single layer and bilayer in P(HOSt-*co*-tBA) film samples at temperature 90 °C (a) and in MG-1 film samples at temperature 70 °C (b). The initial PAG loading for top layer of the bilayer and the single layer are 2 % and 5 % by mass for (a) and (b), respectively. Exposure dose is ≈ 150 mJ/cm^2. The solid lines are fitted curves with kinetics model.

Table III. Reaction rate constants, trapping constants and diffusion coefficients for in P(HOSt-*co*-tBA)[1]

	Top/Bottom layer (nm)	k_P (nm^{3}s^{-1})	k_T (s^{-1})	D_H (nm^2/s)
Thin film; 2% PAG	64.8 / 89.1	0.48	0.0267	4.5
Thick film; 2% PAG	69.0 / 211.2	0.47	0.0279	4.1
Thick film; 5% PAG	71.1 / 222.3	0.58	0.0304	3.9
Average[2]		0.51 ±0.06	0.028±0.002	4.2 ± 0.3

[1]PEB temperature of 90 °C. The single layer film is also prepared through PDMS film transfer technique.
[2]average of three values with uncertainty given as one standard deviation.

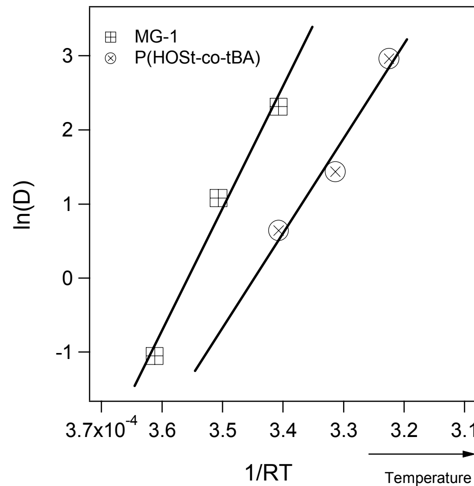

Figure 5. The natural logarithm of measured photoacid diffusion coefficients for MG and P(HOSt-*co*-tBA) versus inverse PEB temperature. The solid lines are fitted lines with Arrhenius equation.

Compared with the results obtained in single layer film (Table I) and bilayer film (Table III) at the same PEB condition for same photoresist, the reaction rate constants k_P are very close showing agreement between two methods, while the discrepancy in k_L and k_T reflect only the difference in the modeling. The temperature dependence of the diffusion

coefficients measured for P(HOSt-*co*-tBA) and MG-1 are shown in Figure 5. The Arrhenius prefactor and activation energy from the are listed in Table IV.

Same as figure 3, figure 5 shows MG-1 resist has larger diffusion coefficient than P(HOSt-*co*-tBA) at the same PEB temperature. This is obviously due to the same mechanism described above. In addition, Table IV also shows that MG-1 has larger prefactor and activation energy than polymeric resist PBOCSt within experimental error, a similar phenomena as we have seen in reaction rate constants if the difference in the kinetics modeling between the author and the literature is not a factor.

The FTIR approach in this study provides a simple but indirect methodology to measure photoacid diffusion coefficients. A more direct method is through the interface reaction front measurement with neutron reflectivity[17]. Our previous study[18] with P(HOSt-*co*-tBA) has shown that the photoacid diffusion constant is ≈ 1.3 nm^2/s at 90 °C PEB, which is in good agreement with these measurements under similar experimental conditions 4.2 nm^2/s. The discrepancy most likely is due to the difference in acid feeder layer diffusion media.

Table IV. Activation energy of photoacid diffusion coefficients of PFBS in P(HOSt-*co*-tBA) and MG-1.

	Prefactor	Activation energy (kJ/mol)
P(HOSt-*co*-tBA)	44 ± 8	127 ± 25
MG-1	59 ± 8	165 ± 23
PBOCSt[16] (Houle et al..)	51.3	152.6

3.3 Diffusion length and deprotection gradient

The photoacid diffusion length is a crucial parameter in order to determine resolution limits with chemically amplified photoresists. The model bilayer technique prepared with the PDMS stamping methods provides a means to determine the optimum diffusion length corresponding to an initial sharp aerial image. This length can be obtained by subtracting the bottom layer film thickness after PEB and development from its original thickness measured with ellipsometry. On the other hand, this diffusion length can also be easily calculated from the kinetics model and the fitted kinetics parameters in which the diffusion length corresponds to the distance from the initial sharp interface of a bilayer to the intersection between the solubility switch and the deprotection profile as shown in Figure 6a. By comparing the calculated and the measured diffusion length, we can validate the kinetics model and the parameters. In addition, we can also calculate the deprotection gradient at the solubility switch, which correlated with LER[19]. The measured and predicted diffusion length and calculated deprotection gradient are all listed in Table V for MG-1 and P(HOSt-*co*-tBA) at several PEB temperature.

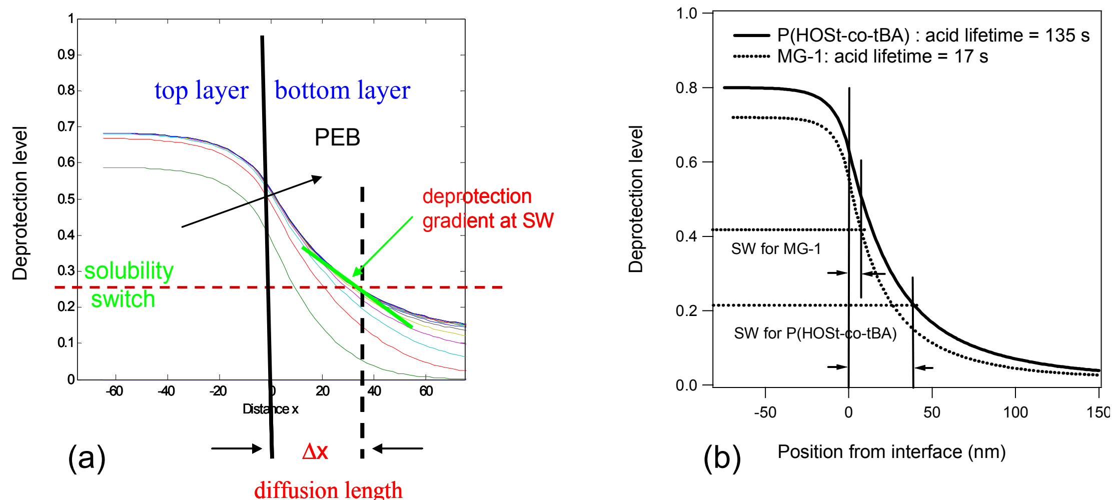

Figure 6. (a) Calculated deprotection profile for P(HOSt-co-tBA) at 90 °C PEB temperature for various PEB time. PAG loading in acid feeding layer is 5% by mass fraction. (b) Calculated deprotection profile for P(HOSt-co-tBA) and MG-1 at 80 °C PEB temperature for 30 min PEB time. PAG loading and dose condition are same as (a) for both resists.

First it can be seen that the measured and calculated diffusion length agree very well with a fitted solubility switch. This shows strong evidence for the applicability of the kinetics model and parameters. For these model conditions of 30 min PEB time, there appears to be a weak dependence on PEB temperature for the diffusion length and deprotection gradient at same PAG loading. Under these conditions even though the initial PAG gradient is sharp the reaction does not proceed to completely deprotect both layers. The reaction becomes pinned such that the reaction front[5,20] essentially stops propagating due to the afore-mentioned trapping effect. Short PEB times would show strong temperature dependence. The PFBS has a significantly smaller diffusion length in the molecular glass than polymer resist matrix. Simultaneously, the deprotection gradient at the solubility switch is larger for the molecular glass at the same PEB temperature. The large difference in diffusion length is attributed to the higher solubility switch for molecular glass which intercepts the deprotection profile at a shorter distance, when compared to the P(HOSt-*co*-tBA) (see Figure 6b). Another reason is that the MG-1 has a larger photoacid trapping effect which results in a shorter acid lifetime even though the diffusion coefficient and reaction rate constant are also larger. Therefore it is a combination of reaction-kinetic parameters and position of the solubility switch that determines the relevant acid diffusion length. A conversion of the diffusion constant to a diffusion length using $l_d = (6*D*t)^{0.5}$ differs from the diffusion length defined as the change in thickness after development of the bilayer. Here we have seen that the diffusion length is not a simple function of diffusion coefficient as we usually thought.

Table V. Diffusion length and deprotection gradient for MG-1 and P(HOSt-*co*-tBA)

P(HOSt-*co*-tBA)			Molecular glass (MG-1)		
PEB[1,2] (°C)	Diffusion length (measured / predicted) (nm)	Deprotection gradient[3] (nm^{-1})	PEB [°C]	Diffusion length (measured / predicted) (nm)	Deprotection gradient [3] (nm^{-1})
80	42 / 38	0.005	60	4 / 5	0.022
90	48 / 45	0.005	70	6 / 7	0.013
100	(29) / (31)	0.004	80	8 / 7	0.016

[1]The PAG loading is 5% PAG (or 2% in parenthesis) in acid feeder layer.
[2] PEB time is ≈ 30 min
[3] The solubility switch is fitted to be 0.22 for polymer resist and 0.42 for MG

3.4 Simulation and Comparison of latent image

To demonstrate validity of the kinetics model parameters obtained with this methodology to a real system, a simulation is conducted and compared with AFM latent image of EUV exposed isolated line before development [21] (figure 7a).

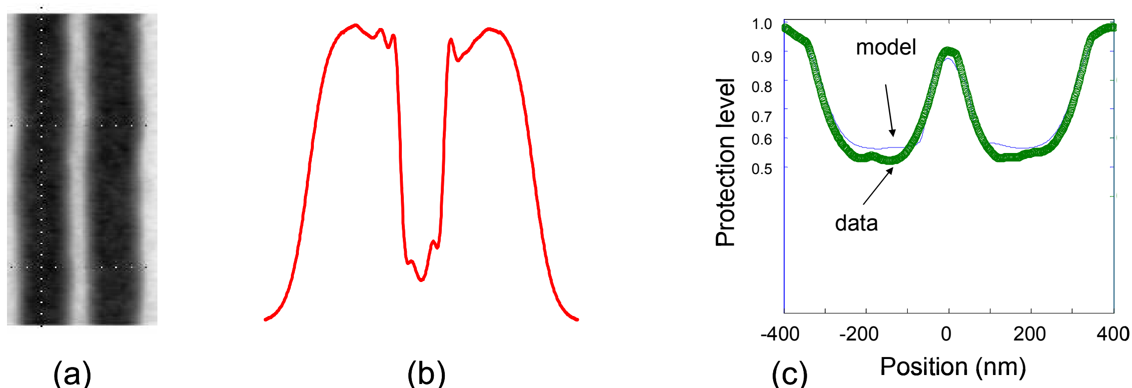

Figure 7. (a) AFM latent image of EUV P(HOSt-co-tBA) resist pattern (100 nm isolated line); Apparent dose is 8 mJ/cm^2 (b) aerial image intensity profile of 100 nm line; (c) Comparison of calculated/model (solid lines) and measured/data (dots) protection profile. The film thickness shrinkage ratio used in protection level conversion from AFM topography data is measured to be 0.243 for 100% deprotection level. An apparent Dill parameter of 0.212 is fitted from four isolated line patterns with four different doses.

Since the film thickness shrinkage induced by outgassing is generally proportional to local deprotection level, the cross-section of latent image can be converted to deprotection profile and compared with the simulated deprotection profile. The intial photoacid distribution used in the modeling can be calculated from Dill's equation with the EUV aerial image profile (Figure 7b) obtained and a fitted Dill's parameter. By applying the intial photoacid distribution and the measured kinetics parameters for the same PEB conditions into equation (1) – (3), we can calculate expected protection profile across the 100 nm isolated line. The result is shown in Figure 7c together with the protection profile converted from AFM latent image (measured/data) with simulated protection profile . The agreement between measured and simulated (calculated) latent image is excellent, suggesting that kinetic model parameters extracted using this methodology can represent a real system and would be useful in photoresist design, processing condition optimization and optical proximity correction.

4. CONCLUSIONS

A quantitative comparison was made between model EUV molecular glass and a polymeric photoresists. It is found that three parameters charactering the reaction-diffusion kinetics of photoacid in photoresists: reaction rate constant, trapping/loss constant and the diffusion constant are all significantly larger in the molecular glass at equal PEB temperature and their sensitivity to PEB is also higher. This has been attributed to the lower glass transition temperature and/or the weaker interaction of photoacid with the resist molecules of MG-1 than in P(HOSt-*co*-tBA).

A methodology to accurately determine acid diffusion coefficients has been proposed and the predicted diffusion length agrees with the measured ones. This methodology is based on a specially prepared model bilayer film with PDMS stamping technique, which not only generates same diffusion media with sharp initial acid distribution, but also is applicable to the situation with base quencher and extendable to any other chemically amplified resist system. In addition, we have also demonstrated that the EUV latent image can be simulated with the measured kinetics parameters. This could be very useful for future resist design, processing condition optimization and optical proximity correction.

5. ACKNOWLEDGEMENTS

This work was supported by a cooperative research and development agreement between Intel Corporation and NIST (NIST CRADA 1893). We also would like to acknowledge Manish Chandhok, Wang Yueh, Todd Younkin, Melissa Shell, Michael Leeson, George Thompson, and Christof Krautschik from Intel, and Chris Soles from NIST for their support. Jim Sounik, Matthew Romberger, and Michael Sheehan at DuPont Electronic Materials provided the polymer used in this study.

6. REFERENCES

[1] Choi, K. W., Prabhu, V. M., Lavery, K. A., Lin, E. K., Wu, W. L., Woodward, JT, Leeson, M., Cao, H., Chandhok, M., and Thompson, G.,"Effect of photo-acid generator concentration and developer strength on the patterning capabilities of a model EUV photoresist," Proceedings of SPIE 6519, 651943 (2007).

[2] Dai, J. Y., Chang, S. W., Hamad, A., Yang, D., Felix, N., and Ober, C. K.,"Molecular glass resists for high-resolution patterning," Chemistry of Materials 18(15), 3404 (2006).

[3] Lavery, K. A., Vogt, B. D., Prabhu, V. M., Lin, E. K., Wu, W. L., Satija, S. K., and Choi, K. W.,"Exposure dose effects on the reaction-diffusion process in model extreme ultraviolet photoresists," Journal of Vacuum Science & Technology B 24(6), 3044 (2006).

[4] Lavery, K. A., Choi, K. W., Vogt, B. D., Prabhu, V. M., Lin, E. K., Wu, W. L., Satija, S. K., Leeson, M., Cao, H., Thompson, G., Deng, H., and Fryer, D. S.,"Fundamentals of the Reaction-Diffusion Process in Model EUV Photoresists," Proceedings of SPIE 6153, 615313 (2006).

[5] Vogt, B. D., Kang, S., Prabhu, V. M., Lin, E. K., Satija, S. K., Turnquest, K., and Wu, W.,"Measurements of the Reaction-Diffusion Front of Model Chemically Amplified Photoresists with Varying Photoacid Size," Macromolecules 39(24), 8311 (2006).

[6] Kang, Shuhui, Prabhu, Vivek M., Vogt, Bryan D., Lin, Eric K., Wu, Wen li, and Turnquest, Karen,"Effect of copolymer composition on acid-catalyzed deprotection reaction kinetics in model photoresists," Polymer 47(18), 6293 (2006).

[7] Kang, Shuhui, Prabhu, Vivek M., Vogt, Bryan D., Lin, Eric K., Wu, Wen li, and Turnquest, Karen,"Copolymer fraction effect on acid catalyzed deprotection reaction kinetics in model 193 nm photoresists," 6153, 61533N (2006).

[8] Kang, S, Vogt, B. D., Wu, W. L., Prabhu, V. M., VanderHart, D. L., Rao, A., Lin, E. K., and Turnquest, K,"Characterization of compositional heterogeneity in chemically amplified photoresist polymer thin films with infrared spectroscopy," Macromolecules 40, 1497 (2007).

[9] Kang, S, Vogt, B. D., Wu, W. L., Prabhu, V. M., VanderHart, D. L., Rao, A., Lin, E. K., and Turnquest, K,"FTIR measurements of compositional heterogeneities," 6159, 615916 (2007).

[10] Krasnoperova, A. A., Khan, M., Rhyner, S., Taylor, J. W., Zhu, Y., and Cerrina, F.,"Modeling and simulations of positive chemically amplified photoresits for x-ray lithography," Journal of Vacuum Science & Technology B 12(6), 3900 (1994).

[11] Zuniga, M. and Neureuther, A.,"Reaction-diffusion modeling and simulations in positive deep ultraviolet resists," Journal of Vacuum Science & Technology B 13(6), 2957 (1995).

[12] Vogt, B. D., Kang, S., Prabhu, V. M., Lin, E. K., Satija, S. K., Turnquest, K., and Wu, W. L.,"Measurements of the reaction-diffusion front of model chemically amplified photoresists with varying photoacid size," Macromolecules 39(24), 8311 (2006).

[13] Lee, J., Park, K., Chang, T., and Jung, J.,"Polymer/probe interaction in probe diffusion through a polymer matrix," Macromolecules 25, 6977 (1992).

[14] Nakamura, J., Ban, H., and Tanaka, A.,"Effect of acid diffusion on performance in positive deep ultravoilet resists," Journal of Vacuum Science & Technology B 12(6), 3888 (1992).

[15] Nakamura, J., Ban, H., and Tanaka, A.,"Influence of acid diffusion on the lithographic performance of chemically amplified resists," Jpn.J.Appl.Phys. 31, 4294 (1992).

[16] Houle, F. A., Hinsberg, W. D., Morrison, M., Sanchez, M. I., Wallraff, G., Larson, C., and Hoffnagle, J.,"Determination of coupled acid catalysis-diffusion processes in a positive-tone chemically amplified photoresist," Journal of Vacuum Science & Technology B 18(4), 1874 (2000).

[17] Lin, E. K., Soles, C. L., Goldfarb, D. L., Trinque, B. C., Burns, S. D., Jones, R. L., Lenhart, J. L., Angelopoulos, M., Willson, C. G., Satija, S. K., and Wu, W. L.,"Direct Measurement of the Reaction Front in Chemically Amplified Photoresists," Science 297, 372 (2002).

[18] Lavery, K. A., Vogt, B. D., Prabhu, V. M., Lin, E. K., Wu, W. L., Satija, S. K., and Choi, K. W.,"Exposure dose effects on the reaction-diffusion process in model extreme ultraviolet photoresists," Journal of Vacuum Science & Technology B 24(6), 3044 (2006).

[19] Pawloski, AR, Acheta, A, Lalovic, I, LaFontaine, B, and Levinson, HJ,"Characterization of line edge roughness in photoresist using an image fading technique," Proceedings of the SPIE, Advances in Resist Technology and Processing XXI 5376, 414 (2004).

[20] Vogt, B. D., Kang, S., Prabhu, V. M., Rao, A., Lin, E. K., Satija, S. K., Turnquest, K., and Wu, W.,"The deprotection reaction front profile in model 193nm methacrylate-based chemically amplified photoresists," 6153, 615316 (2006).

[21] Woodward, J. T., Choi, K. W., Prabhu, V. M., Kang, S., Prabhu, V. M., Lavery, K., Wu, W., Leeson, M., Silva, A. D., Felix, N. M., Ober, C. K. "Characterization of the latent image to developed image in model EUV photoresists" SPIE 2008. In preparation.